RESEARCH ARTICLE

# Refining the Balance of Attenuation and Immunogenicity of Respiratory Syncytial Virus by Targeted Codon Deoptimization of Virulence Genes

**Jia Meng,[a,b] Sujin Lee,[a,b] Anne L. Hotard,[a,b] Martin L. Moore[a,b]**

Department of Pediatrics, Emory University School of Medicine, Atlanta, Georgia, USA[a]; Children's Healthcare of Atlanta, Atlanta, Georgia, USA[b]

**ABSTRACT** **Respiratory syncytial virus (RSV) is the most important pathogen for lower respiratory tract illness in children for which there is no licensed vaccine. Live-attenuated RSV vaccines are the most clinically advanced in children, but achieving an optimal balance of attenuation and immunogenicity is challenging. One way to potentially retain or enhance immunogenicity of attenuated virus is to mutate virulence genes that suppress host immune responses. The NS1 and NS2 virulence genes of the RSV A2 strain were codon deoptimized according to either human or virus codon usage bias, and the resulting recombinant viruses (dNSh and dNSv, respectively) were rescued by reverse genetics. RSV dNSh exhibited the desired phenotype of reduced NS1 and NS2 expression. RSV dNSh was attenuated in BEAS-2B and primary differentiated airway epithelial cells but not in HEp-2 or Vero cells. In BALB/c mice, RSV dNSh exhibited a lower viral load than did A2, and yet it induced slightly higher levels of RSV-neutralizing antibodies than did A2. RSV A2 and RSV dNSh induced equivalent protection against challenge strains A/1997/12-35 and A2-line19F. RSV dNSh caused less STAT2 degradation and less NF-κB activation than did A2 *in vitro*. Serial passage of RSV dNSh in BEAS-2B cells did not result in mutations in the deoptimized sequences. Taken together, RSV dNSh was moderately attenuated, more immunogenic, and equally protective compared to wild-type RSV and genetically stable.**

**IMPORTANCE** **Respiratory syncytial virus (RSV) is the leading cause of infant viral death in the United States and worldwide, and no vaccine is available. Live-attenuated RSV vaccines are the most studied in children but have suffered from genetic instability and low immunogenicity. In order to address both obstacles, we selectively changed the codon usage of the RSV nonstructural (NS) virulence genes NS1 and NS2 to the least-used codons in the human genome (deoptimization). Compared to parental RSV, the codon-deoptimized NS1/NS2 RSV was attenuated *in vitro* and in mice but induced higher levels of neutralizing antibodies and equivalent protection against challenge. We identified a new attenuating module that retains immunogenicity and is genetically stable, achieved through specific targeting of nonessential virulence genes by codon usage deoptimization.**

**Received** 24 July 2014 **Accepted** 2 September 2014 **Published** 23 September 2014

**Citation** Meng J, Lee S, Hotard AL, Moore ML. 2014. Refining the balance of attenuation and immunogenicity of respiratory syncytial virus by targeted codon deoptimization of virulence genes. mBio 5(5):e01704-14. doi:10.1128/mBio.01704-14.

**Editor** Jack R. Bennink, National Institute of Allergy and Infectious Diseases



Address correspondence to Martin L. Moore, martin.moore@emory.edu.

Respiratory syncytial virus (RSV) is the leading cause of lower respiratory tract illness (LRTI) in young children, manifested as bronchiolitis and pneumonia. In the United States, there are 132,000 to 172,000 estimated annual RSV-associated hospitalizations in children less than 5 years of age, with the highest hospitalization rates seen in very young infants (1). RSV-associated LRTI results in an annual 66,000 to 199,000 deaths in children younger than 5 years old globally (2). Prophylaxis currently available to prevent RSV-associated disease is a humanized monoclonal antibody (palivizumab) targeting the RSV fusion (F) protein, but it is prescribed only to infants with certain risk factors (prematurity, congenital heart disease, and congenital pulmonary dysplasia) (3), underscoring its limited use. Developing safe and effective vaccines against RSV faces many challenges (reviewed in references 4 and 5).

RSV is a member of the *Paramyxoviridae* family, which contains important human pathogens. RSV carries 10 genes from which 11 proteins are produced. Two promoter-proximal nonstructural (NS1 and NS2) proteins inhibit interferon (IFN) pathways, including type I and type III IFN and potentially type II IFN (6–14). NS1 and NS2 exert their immune-suppressive functions on human dendritic cells (DC) as well as $CD4^+$ and $CD8^+$ T cells (15–17). NS1 and NS2 have also been shown to inhibit apoptosis in infected cells to facilitate viral growth (18). Deletion of either NS1 or NS2 results in virus attenuation, while simultaneously deleting both NS1 and NS2 overattenuates the virus for vaccine purposes (19–22). Combined with other attenuating cold-passage (*cp*) and/or temperature-sensitive (*ts*) point mutations, viruses with ΔNS1 or ΔNS2 were evaluated as potential live-attenuated vaccine candidates, and ΔNS1 was highly attenuated, whereas ΔNS2 was underattenuated (19, 20, 22–24). Deletion of nonessential virulence genes provides a limited range of attenuation. Another challenge associated with setting the attenuation level of live-attenuated vaccines containing *cpts* point mutations is reversion or compensatory mutations. This is especially the case for RNA viruses (23, 25, 26), highlighting the need to further stabilize

vaccine candidates. Attenuating mutations can also be associated with loss of immunogenicity due to reduced replicative fitness, as seen with RSV rA2ΔM2-2 (19, 27).

The codon usage deoptimization strategy was first used to address the problem of genetic instability of live-attenuated poliovirus vaccines (28, 29). Codon deoptimization of the poliovirus capsid gene by incorporation of the rarest codons in the human genome reduced translation of capsid protein, resulting in virus attenuation (28, 29). Another attenuation strategy, codon pair deoptimization, has been used to recode viral genes using rare codon pairs, which does not necessarily alter codon usage (30). In this study, we applied codon usage deoptimization combined with selective targeting of viral immune-suppressive genes to a human pathogen and characterized the genetic stability, replicative fitness, immunogenicity, and protective efficacy of the recoded virus. To our knowledge, this is the first example of virus attenuation by codon deoptimization specifically of nonessential virulence genes. Our results demonstrate that targeting RSV NS1 and NS2 by codon deoptimization can be an effective strategy for developing live-attenuated vaccines with controllable attenuation, wild-type replication in Vero cells, genetic stability, and improved immunogenicity.

## RESULTS

**Generation of codon-deoptimized NS1 and NS2 RSV.** We compared codon usage in the NS1 and NS2 genes of several RSV strains to the codon usage bias of the human genome (31). Of the 18 amino acids used in the RSV NS1 and NS2 genes, 6 (33%) share the same least-used codons as those of human genes. Therefore, because we could not rule out the possibility that RSV utilizes a unique codon usage bias, we designed two mutant viruses with codon-deoptimized NS1 and NS2 genes, namely, dNSh (wherein every codon in NS1 and NS2 is the least used for that amino acid in humans) and dNSv (all NS1 and NS2 codons are the least used by RSV). The dNSh design included 84 silent mutations in NS1 and 82 in NS2, the dNSv design included 145 silent mutations for NS1 and 103 mutations for NS2, and these nucleotide changes were distributed across the coding regions for both genes (Fig. 1). Wild-type NS1 and NS2 genes were replaced by deoptimized NS1 and NS2 genes using MscI and EcoRV sites (Fig. 2). The kRSV-dNSh and kRSV-dNSv mutants (k designates inclusion of the far-red fluorescent protein mKate2 in the first gene position, as described previously [32]) were rescued by reverse genetics, and the sequences of NS1 and NS2 genes were confirmed for all viral stocks. To test the genetic stability of the human codon-deoptimized virus, we serially passaged the virus in three separate lines in BEAS-2B cells at 37°C for 10 passages and sequenced the final passage stocks (P10). All three P10 lines maintained the original deoptimized sequences for both NS1 and NS2 genes.

**Reduced NS1 and NS2 protein expression by kRSV-dNSh *in vitro*.** In order to examine the effect of codon deoptimization on NS1 and NS2 expression, HEp-2, BEAS-2B, and Vero cells were infected at a multiplicity of infection (MOI) of 5 with either parental kRSV-A2 or deoptimized virus kRSV-dNSh or kRSV-dNSv. Twenty-four hours postinfection (p.i.), total cell lysates were harvested and analyzed by Western blotting (Fig. 3). Relative steady-state NS1 and NS2 levels were determined by densitometry. Compared to kRSV-A2, human-codon-bias-deoptimized virus (kRSV-dNSh) expressed 75 to 90% less NS1 protein and 70 to 90% less NS2 protein in these cell lines (Fig. 3). In contrast, RSV-codon-bias-deoptimized virus (kRSV-dNSv) expressed higher levels of NS1 and NS2 than did the parental virus, especially in HEp-2 and Vero cell lines (Fig. 3A and C). As the kRSV-dNSh virus exhibited the desired phenotype of reduced NS1 and NS2 levels, we chose this mutant for further studies.

***In vitro* replication of human-deoptimized NS1/NS2 RSV.** Multistep growth curve analyses were done in several cell lines as well as primary, normal human bronchial epithelial (NHBE) cells differentiated at the air-liquid interface (ALI). kRSV-dNSh grew to similar levels as kRSV-A2 in HEp-2 and Vero cell lines (Fig. 4A and B). In BEAS-2B cells, the two viruses replicated to similar levels at earlier time points p.i., but growth of kRSV-dNSh was attenuated at 72 and 96 h p.i. (Fig. 4C). Primary differentiated airway epithelial cells provide a more accurate model than immortalized continuous cell lines for rank ordering RSV attenuation levels (33). We therefore compared the growth kinetics of kRSV-dNSh and kRSV-A2 in differentiated NHBE/ALI cultures. At MOIs of 0.2 and 2.0, kRSV-dNSh virus exhibited a more restricted growth phenotype in these cell cultures, unlike kRSV-A2, which maintained its replication throughout the experiments (Fig. 4D to F). Although the two viruses started with similar levels of infection (Fig. 4F, day 1), only kRSV-A2 infectious yield increased (Fig. 4F). Similarly to previously published data, the RSV-infected NHBE cells exhibited no obvious cytopathic effect over the course of infection (Fig. 4F) (34).

**Attenuation, protection, and immunogenicity in BALB/c mice.** BALB/c mice were infected with either kRSV-A2 or kRSV-dNSh virus, and lung viral loads were measured at indicated days postinfection. Both viruses peaked between days 4 and 6, and kRSV-dNSh exhibited approximately a 1-$\log_{10}$-lower titer than kRSV-A2 on both days (Fig. 5A). As complete protection against RSV challenge is commonly achieved in the BALB/c mouse model with experimental RSV vaccines, we increased the stringency of efficacy determination in this model by using a dose titration of vaccines to evaluate breakthrough of protection. When given as a single vaccination of $10^5$ fluorescent focus units (FFU) intranasally (i.n.), both kRSV-A2 and kRSV-dNSh elicited complete protection against heterologous subgroup A RSV strain A/1997/12-35 (12-35 [35]) challenge at 100 days postvaccination (Fig. 5B). Vaccination using kRSV-A2 or kRSV-dNSh with $10^4$ or $10^3$ FFU resulted in equivalent levels of protection and breakthrough. This protection correlated with induction of RSV-neutralizing antibodies (nAb) over time, and kRSV-dNSh induced slightly but statistically significantly higher levels of nAb than did kRSV-A2 (Fig. 5C). Mice vaccinated with a dose range of either kRSV-A2 or kRSV-dNSh also showed similar levels of protection against challenge with RSV A2-line19F at day 28 postvaccination (Fig. 5D). Taken together, kRSV-dNSh was significantly attenuated in mice but was equally protective and slightly more immunogenic than the parental kRSV-A2 strain.

**STAT2 degradation and NF-κB activation.** We characterized the effect of kRSV-dNSh infection on STAT2, a known target for NS2 and potentially NS1 (6, 7, 9, 10, 13). 293T cells were mock infected or infected with either wild-type kRSV-A2 or kRSV-dNSh. As expected, kRSV-A2 infection caused 50% STAT2 degradation compared to mock infection. In contrast, we found that kRSV-dNSh infection had no effect on STAT2 levels compared to mock infection (Fig. 6A), suggesting that reduced NS1 and NS2 protein levels may augment host immune responses due to less STAT2 degradation compared to wild-type virus infection.

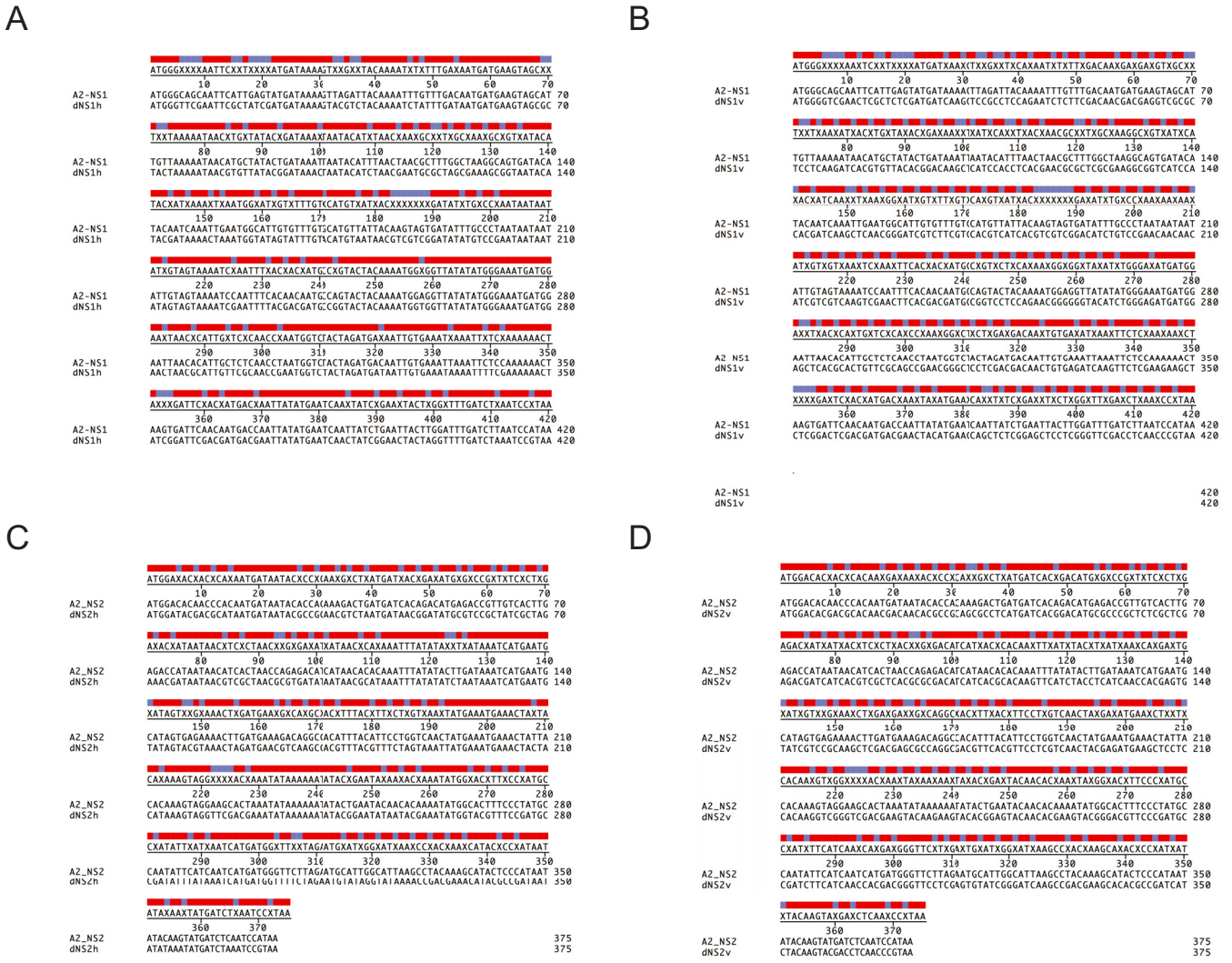


**FIG 1** (A and B) Nucleotide sequence alignment of RSV A2 strain NS1 open reading frame (ORF) with human-codon-deoptimized NS1 (dNS1h) (A) or virus-codon-deoptimized NS1 (dNS1v) (B) ORF. (C and D) Nucleotide sequence alignment of RSV A2 strain NS2 ORF with human-codon-deoptimized NS2 (dNS2h) (C) or virus-codon-deoptimized NS2 (dNS2v) (D) ORF. Nucleotide changes compared to A2 are highlighted in blue in the consensus sequences.

Early during RSV infection, NS1 and NS2 proteins activate host cell prosurvival signals to promote viral growth, including NF-κB, so that NF-κB activation is a measure of NS1/NS2 function (12, 18). Activation of NF-κB leads to expression of proinflammatory cytokines. Pediatric live-attenuated vaccine strains should preferably be less proinflammatory than wild-type strains for safety concerns. HEK-Blue-Null 1 cells, which contain an NF-κB reporter gene, were mock infected or infected with kRSV-A2 or kRSV-dNSh. Tumor necrosis factor alpha (TNF-α), as a positive control for NF-κB activation, induced a high level of reporter activity, followed by kRSV-A2 virus infection (Fig. 6B). Mock infection and kRSV-dNSh infection resulted in equivalent low levels of NF-κB activation, indicating a reduced NF-κB activation and inflammatory potential of kRSV-dNSh compared to the wild-type virus.

## DISCUSSION

Here, we adapted the codon deoptimization strategy to specifically target RSV nonessential virulence genes NS1 and NS2, which function in immune suppression. Deoptimization was based on human codon usage bias, which resulted in reduced target protein expression. Unlike previous RSV attenuation strategies focusing on virus replication *per se*, diminishing expression of NS1 and NS2 led to attenuation without loss of immunogenicity or infectious yield in Vero cells. Codon deoptimization of nonessential target virulence genes can simultaneously fine-tune attenuation and immunogenicity. The stability of the recoded sequences was also confirmed by *in vitro* passaging the virus stocks in a restrictive cell line (BEAS-2B) without new mutations.

NS1 and NS2 proteins of RSV suppress type I and type III IFN responses in human epithelial cells and macrophages and have similar effects on mouse cells (11, 13, 15). Homologous genes in related viruses, pneumonia virus of mice (PVM) and bovine respiratory syncytial virus (BRSV), also antagonize type I and type III IFN responses (36–39). Targets of NS1 and NS2 genes include various members of the type I IFN pathways, including STAT2 (6–10, 13, 14). In agreement with these studies, we found that

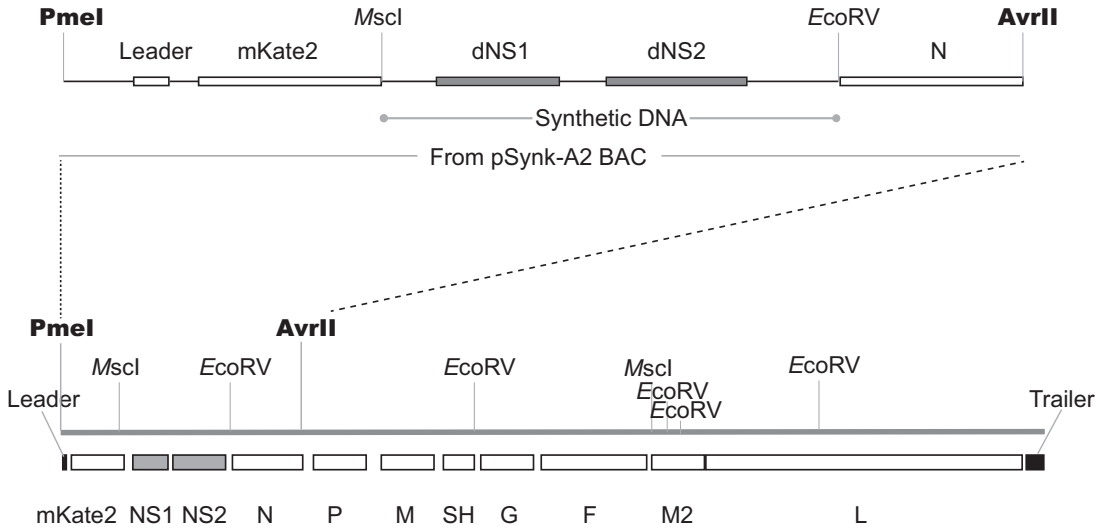


**FIG 2** Generation of recombinant RSV with codon-deoptimized NS1 and NS2. The PmeI-to-AvrII fragment from the parental RSV pSynk-A2 BAC clone was subcloned to replace the NS1 and NS2 regions with synthetic DNA containing the codon-deoptimized NS1 and NS2 using MscI and EcoRV sites.

STAT2 protein levels were reduced in kRSV-A2 infection but not during kRSV-dNSh infection. There is functional overlap between NS1 and NS2 proteins (6, 9, 11, 12, 15, 17). For example, NS1 and NS2 can cooperatively suppress the maturation of dendritic cells (DC), as ΔNS1/NS2 RSV treatment resulted in higher DC maturation than did ΔNS1 or ΔNS2 treatment (17). Both NS1 and NS2 inhibit IRF3 activation in human epithelial cells (12). Both genes inhibit induction of human alpha interferon (IFN-$\alpha$), IFN-$\beta$, and IFN-λ (11). The overlapping functions of NS1 and NS2 could be explained by their potential interaction and formation of multisubunit complexes in the infected cell (7, 13, 40). Collectively, these studies show that double deletion of NS1 and NS2 attenuates the virus more than the single deletions and induces the highest level of antiviral immune responses, supporting our strategy to target both nonstructural genes of RSV.

Deletion of either RSV NS gene or both results in virus attenuation both *in vitro* and *in vivo* (11, 19–22, 41). ΔNS1 and ΔNS2 single deletion mutants and the ΔNS1/NS2 double deletion mutant replicate at lower levels than wild-type virus, with ΔNS2 only slightly attenuated and ΔNS1/2 about 2 $\log_{10}$ attenuated in BALB/c mice (15). We found that kRSV-dNSh virus had a milder phenotype than ΔNS1/2 because kRSV-dNSh was 1 $\log_{10}$ attenuated in mice. This is promising because ΔNS1/2 was overattenuated as a vaccine. Also, kRSV-dNSh virus was not attenuated in Vero cells, the presumed vaccine strain producer cells, unlike ΔNS1/2, which exhibited a 20-fold-lower titer in Vero cells (11).

Transcription factor NF-κB activates many host antiapoptotic and proinflammatory genes and is activated by NS1 and NS2 genes rapidly during RSV infection to delay apoptosis (12, 18). Blocking apoptosis by activation of NF-κB to promote viral replication has been documented for other viruses, such as HIV-1, influenza virus, hepatitis B virus (HBV), and HCV (42). We speculate that reduced NF-κB activation by kRSV-dNSh, compared to kRSV-A2, may contribute to the attenuated phenotype of this mutant due to accelerated cell death (Fig. 6B).

Virus attenuation through manipulation of codon usage or codon pair usage in conjunction with synthetic biology has been achieved for several viruses, including poliovirus and influenza virus (28–30, 43, 44). Rather than recoding the protein sequence by using the rarest codons for each amino acid (codon deoptimization), codon pair deoptimization recodes the protein sequence to maximize the occurrence of the rarest adjacent codon pairs. The mechanisms behind virus attenuation using either method are not completely defined. Decreased translational efficiency of codon-deoptimized or codon pair-deoptimized genes is considered the main principle, although mRNA stability was not examined in each case (28, 30, 43, 44). According to the "mutation-selection-drift balance" model, codon bias may be under weak selection for translation efficiency or accuracy, although other mechanisms are proposed, such as mutational bias (45). Studies of tRNA concentration either by gene copy number or by direct measure of cellular tRNA pools have provided a consistent correlation between tRNA abundance and corresponding codon usage frequency, lending support to translational selection on codon bias (46). Codon usage appears to be an important cellular strategy to control protein expression level, activity, function, and ultimately physiology (47–50). Other than selection on translation efficiency, codon usage pattern has also been implicated in regulating the protein-folding process (50, 51). Thus, the production of a functional protein from mRNA is tightly regulated by its codon usage pattern in every step of the process.

We propose codon deoptimization of nonessential virus virulence genes as a general strategy in generating live-attenuated vaccine candidates with retained immunogenicity *in vivo*, genetic stability, and replication in producer cell lines *in vitro*. This may be important for RSV vaccines because the wild-type virus is not potently immunogenic and does not grow to high titers *in vitro*. Additionally, reversion to wild-type virulence in the context of codon deoptimization is minimized due to the additive contribution of silent mutations across the coding region (30), and our *in vitro* serial passaging experiment provided support for this. Because the recoding method does not change protein sequence, it will maximally preserve immune epitopes. Although more studies are needed to understand the effect of recoding protein sequences

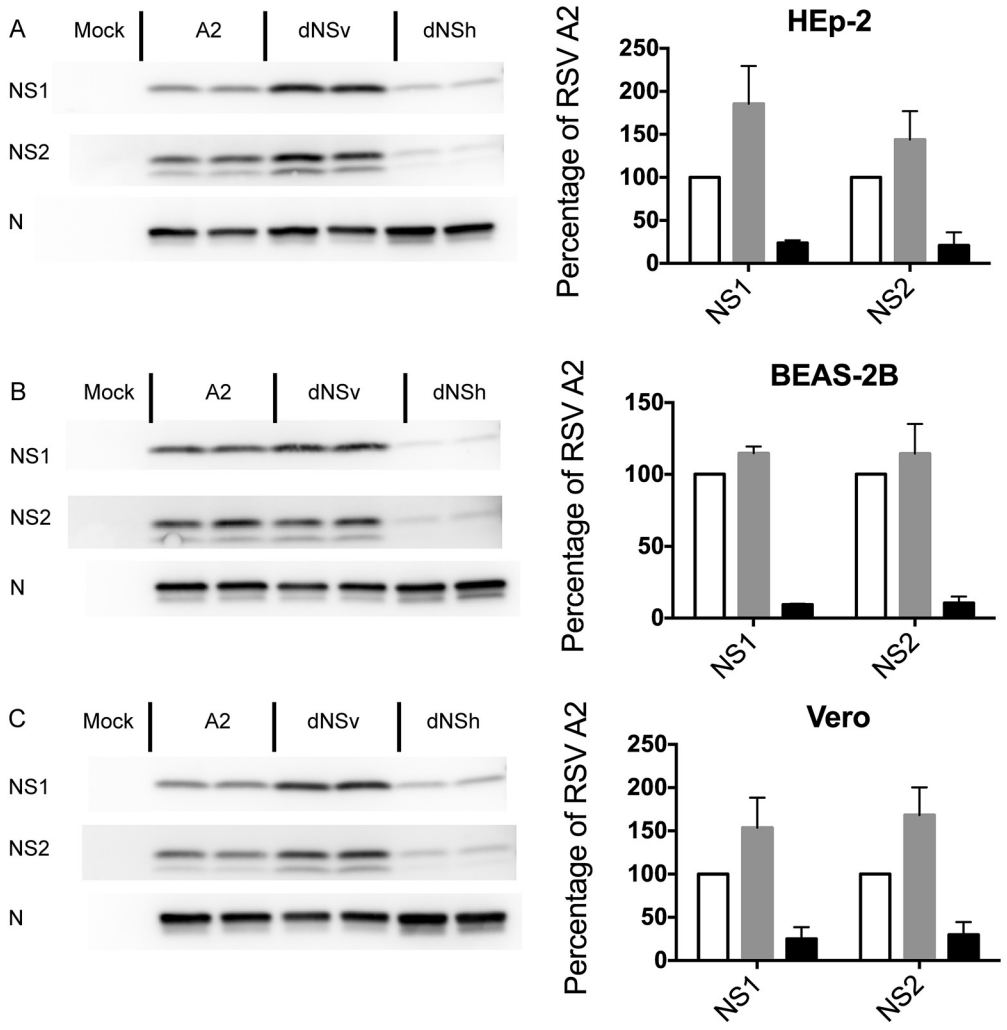


**FIG 3** Expression of NS1 and NS2 proteins during RSV infection in cell lines. HEp-2 (A), BEAS-2B (B), and Vero (C) cells were mock infected or infected with either kRSV-A2, kRSV-dNSv, or kRSV-dNSh at an MOI of 5. Twenty hours p.i., NS1 and NS2 protein levels were analyzed by Western blotting and densitometry. Representative blots are shown on the left. Densitometry results from 2 to 3 independent experiments are shown on the right. After normalization to RSV N protein expression level, NS1 and NS2 protein levels from each virus were normalized to those during kRSV-A2 infection and expressed as percentage ± SD. Unfilled bars represent kRSV-A2, gray bars represent kRSV-dNSv, and black bars represent kRSV-dNSh.

using either rare codons or codon pairs on protein translation, targeting virulence genes using this method should be widely applicable to many viruses for live-attenuated vaccine development.

## MATERIALS AND METHODS

**Cell lines.** Vero (ATCC CCL-81) and HEp-2 (ATCC CCL-23) cells were maintained in minimal essential medium (MEM) with Earle's salts and L-glutamine (Gibco) supplemented with 10% fetal bovine serum (FBS) (HyClone) and 1 $\mu$g/ml penicillin, streptomycin sulfate, and amphotericin B solution (PSA) (Invitrogen). BEAS-2B cells were maintained in RPMI 1640 (Cellgro) with 10% FBS, as described previously (35). HEK-Blue-Null 1 cells, which express secreted embryonic alkaline phosphatase (SEAP) under the control of the IFN-$\beta$ minimal promoter fused to NF-$\kappa$B and AP-1 binding sites, were maintained in Dulbecco's modified Eagle medium supplemented with 10% FBS, L-glutamine, 4.5 g/liter D-glucose, and 1 $\mu$g/ml PSA, as recommended by the provider (InvivoGen, San Diego, CA). BSR-T7/5 cells were a gift from Ursula Buchholz (National Institutes of Health, Bethesda, MD) and were cultured in Glasgow's minimal essential medium (GMEM) containing 10% FBS and 1 $\mu$g/ml PSA. BSR-T7/5 cells were selected with 1 mg/ml Geneticin every other passage.

**RSV strains.** We performed RSV reverse genetics by cotransfection of five plasmids, an RSV antigenomic cDNA cloned in a bacterial artificial chromosome (BAC) and four codon-optimized helper plasmids that express RSV N, P, M2-1, or L protein, into BSR-T7/5 cells as we described previously (32). The pSynkRSV-line19F BAC produces A2-line19F RSV with the far-red fluorescent protein monomeric Katushka-2 (mKate2) in the first position (32) to mark infected cells. We modified pSynkRSV-line19F by replacing the line 19 strain fusion (F) gene, flanked by SacII-to-SalI sites in the BAC, with a synthetic cDNA (GeneArt) containing the A2 strain F open reading frame (A2 from Barney Graham, Vanderbilt University; GenBank accession number FJ614814) flanked by noncoding regions identical to those in pSynkRSV-line19F and corresponding SacII-to-SalI sites (32). The resulting BAC (pSynk-A2) was used as the genetic background for insertion of codon-deoptimized RSV nonstructural (NS) genes. The PmeI-AvrII fragment from pSynk-A2 BAC (Fig. 2) was subcloned. The MscI-to-EcoRV fragment of pSynk-A2 was replaced with a corresponding synthetic fragment (GeneArt, Life Technologies, Gaithersburg, MD) in which only the NS1 and NS2 open reading frames were codon deoptimized based on either human or viral codon usage to generate kRSV-dNSh or kRSV-dNSv, respectively. Recombinant RSV was

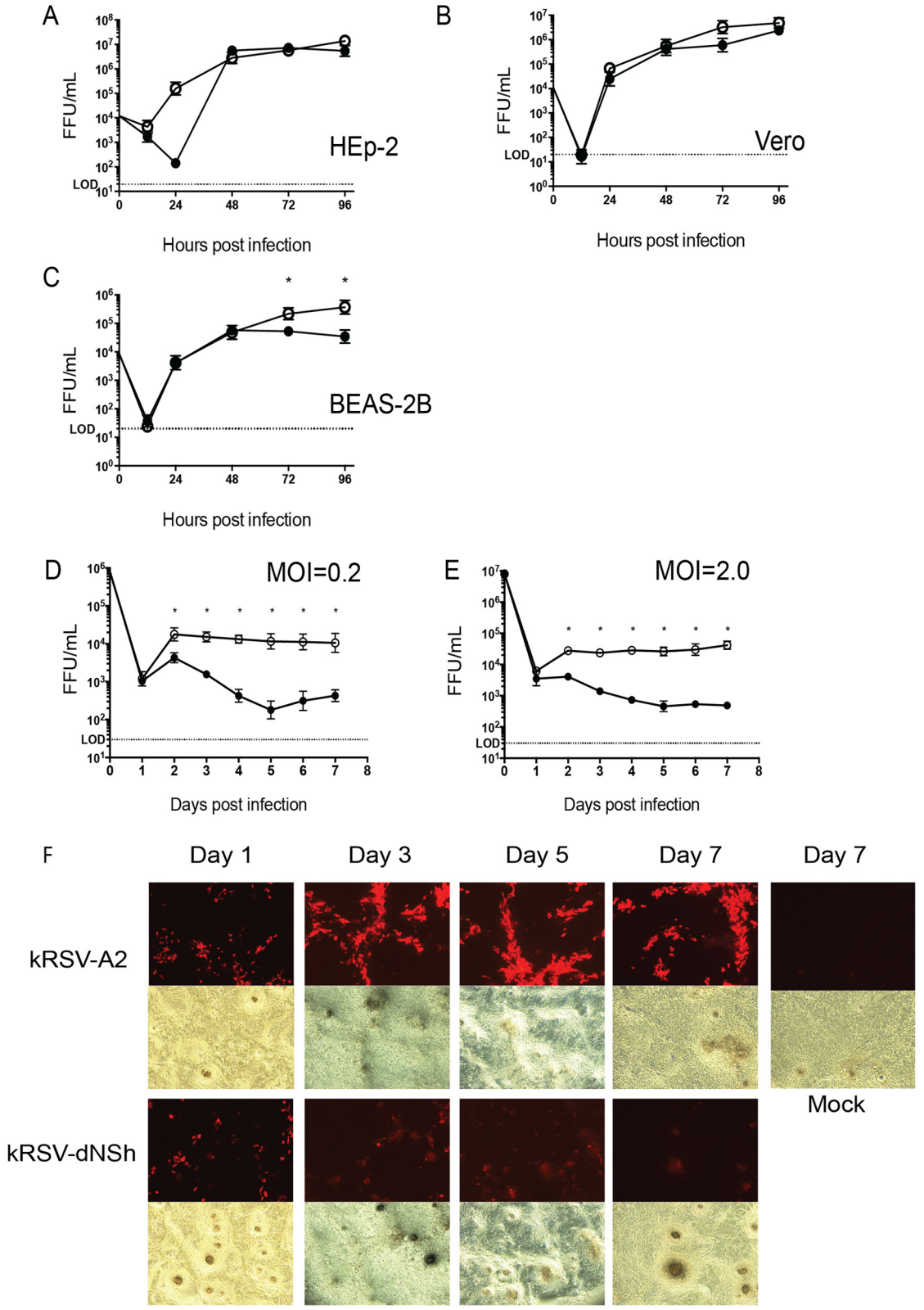


**FIG 4** (A to E) Growth kinetics of kRSV-A2 (open circles) and kRSV-dNSh (closed circles) in HEp-2 (A), Vero (B), and BEAS-2B (C) cells at 37°C infected at an MOI of 0.01, as well as in differentiated NHBE/ALI cells infected at an MOI of 0.2 (D) and 2.0 (E). (F) Time course images for NHBE cells infected at an MOI of 0.2, showing mKate2 fluorescence produced by recombinant viruses. For growth curves in panels A, B, and C, each graph is compiled from two independent experiments performed in duplicate wells. For panels D and E, each single experiment was performed in triplicate wells. *, $P < 0.05$ between kRSV-dNSh- and kRSV-A2-infected groups. NHBE, normal human bronchial epithelial cells; ALI, air-liquid interface; LOD, limit of detection.

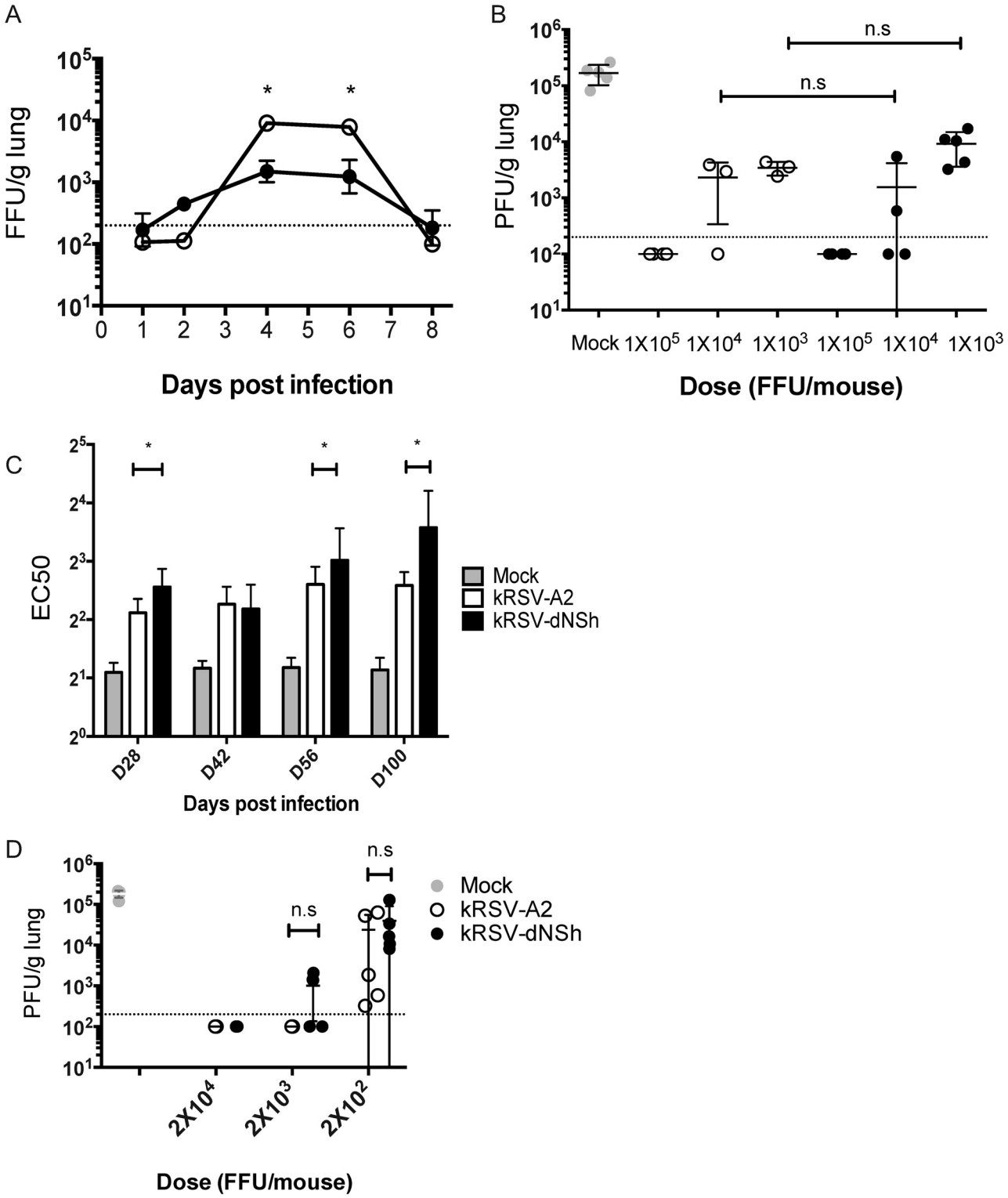


**FIG 5** Attenuation, efficacy, and immunogenicity. (A) BALB/c mice (5 per group) were infected i.n. with either kRSV-A2 (open circles) or kRSV-dNSh (closed circles), and lung viral loads on indicated days are shown. *, $P < 0.05$ comparing kRSV-A2 to kRSV-dNSh at days 4 and 6. (B) BALB/c mice (5 per group) were vaccinated i.n. with various doses of either kRSV-A2 (open circles) or kRSV-dNSh (closed circles) or mock infected (gray circles) and challenged with the RSV 12-35 strain 100 days later. Lung peak viral loads after challenge are shown. Each symbol represents a single mouse. (C) Serum nAb titers measured at indicated days after vaccination with $1 \times 10^5$ FFU. There were 5 mice per group. *, $P < 0.05$ comparing the bracketed kRSV-dNSh- and kRSV-A2-infected groups. (D) Lung peak viral loads after rA2-line19F challenge 28 days postvaccination. Each symbol represents a single mouse. All data represent one of two replicate experiments with similar results. Dotted lines indicate limit of detection for plaque assay. i.n., intranasal; FFU, fluorescent focus unit; PFU, plaque-forming unit; n.s., not significant.

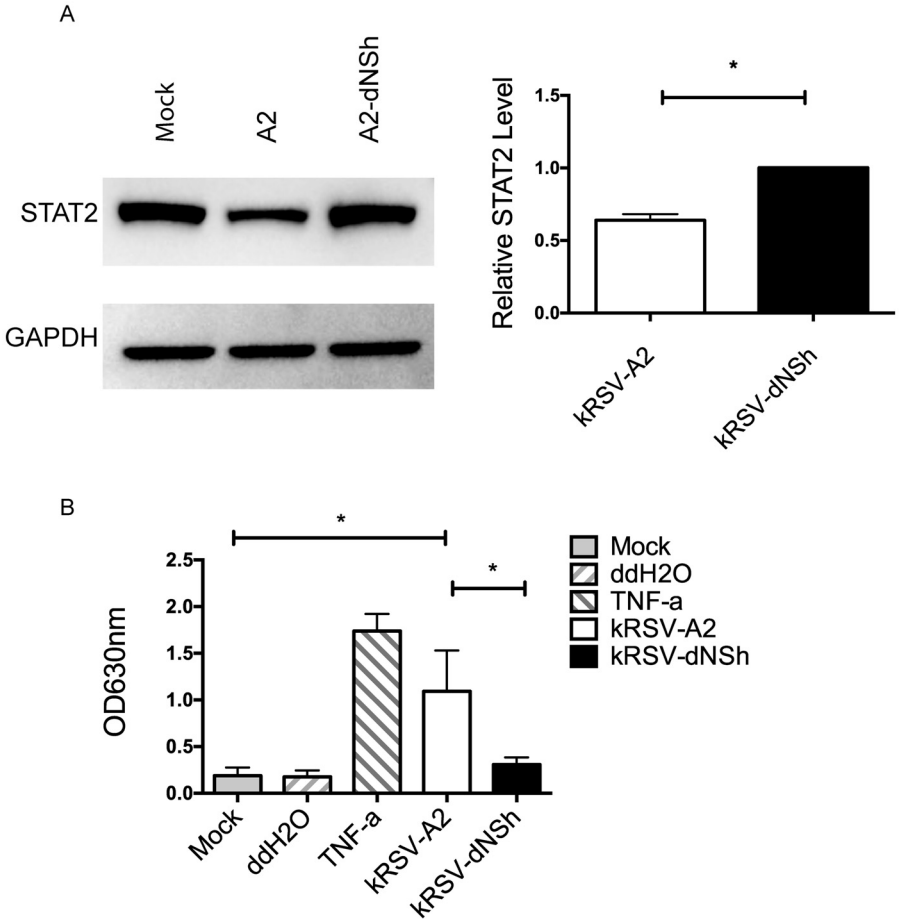


**FIG 6** STAT2 degradation and NF-κB activation. (A) 293T cells infected with either kRSV-A2 or kRSV-dNSh or mock infected at an MOI of 3. Twenty hours p.i., total STAT2 protein level was analyzed by Western blotting and densitometry (from three independent experiments). (B) HEK-Blue-Null 1 cells treated with either kRSV-A2, kRSV-dNSh, mock treatment, TNF-α (1 ng/ml), or double-distilled water ($ddH_2O$) for 72 h. Supernatants were measured for reporter activity using a colorimetric assay (from three independent experiments). *, $P < 0.05$ between the groups indicated by the open brackets.

recovered by transfection as described previously, except that virus stocks were propagated in Vero cells (32). All the virus stocks used in this study were sequenced for the NS1 and NS2 genes and confirmed to be mycoplasma negative using the Venor GeM *Mycoplasma* detection kit (Sigma-Aldrich, St. Louis, MO). Challenge virus strains A2-19F and RSV 12-35 were generated in HEp-2 cells as described previously and titrated by plaque assay on HEp-2 cells (35).

**Normal human bronchial epithelial cells at air-liquid interface (NHBE/ALI).** NHBE cells (Lonza, Allendale, NJ) were cultured according to the recommended protocols. Cells were seeded onto collagen-coated (BD Bioscience, Bedford, MA) 24-well transwell supports (Corning Costar, NY) for differentiation. Briefly, $5 \times 10^4$ cells (100 μl) in B-ALI growth medium (Lonza) were seeded per insert with 500 μl B-ALI growth medium added to the basal chamber. Growth medium in both apical and basal chambers was changed the next day. Air-lift was performed on day 3 by removing B-ALI growth medium from both chambers followed by adding 500 μl B-ALI differentiation medium (Lonza) supplemented with inducer only to the basal chamber. Differentiation medium in the basal chamber was replaced with fresh medium every other day for 21 days before experiments.

**Western blotting.** Cells (HEp-2, Vero, or BEAS-2B) at 70% confluence were infected with kRSV-A2, kRSV-dNSh, or kRSV-dNSv at an MOI of 5, and cell lysates were harvested 20 h p.i. in RIPA buffer (Sigma-Aldrich, St. Louis, MO) containing 1× protease inhibitor cocktail (Thermo Scientific, Rockford, IL). Proteins were separated by SDS-PAGE and transferred onto polyvinylidene difluoride membranes. Blots were blocked with 5% nonfat milk in Tris-buffered saline (TBS) plus 0.1% Tween 20. Polyclonal rabbit antisera against NS1 and NS2 proteins (gifts from Michael Teng, USF Health) were used to quantify protein levels. Blots were stripped and reprobed with a mouse monoclonal antibody against RSV N protein (clone D14, a gift from Edward Walsh) as a loading control. For STAT2 protein detection, 293T cells at 70% confluence were mock infected or infected with either kRSV-A2 or kRSV-dNSh virus at an MOI of 3. Cell lysates were harvested 12 h later. Blots were probed with rabbit anti-STAT2 polyclonal antibody (C20; Santa Cruz Biotechnology, Santa Cruz, CA). Blots were stripped and reprobed with mouse anti-glyceraldehyde-3-phosphate dehydrogenase (anti-GAPDH) antibody (6C5; GeneTex, Irvine, CA) as a loading control.

**FFU assay.** Vero cells at 70% confluence in 96-well plates were inoculated with 50 μl of 10-fold serial dilutions of samples. Inoculation was carried out at room temperature with gentle rocking for 1 h before 0.75% methylcellulose (EMD, Gibbstown, NJ) dissolved in MEM supplemented with 10% FBS and 1% PSA was added. Cells were incubated for 48 h before counting FFU per well. The limit of detection is 1 FFU per well, corresponding to 20 FFU/ml.

**Virus growth kinetics.** Seventy percent confluent cells in 6-well plates were infected at an MOI of 0.01 in a volume of 500 μl. After 1-h incubation at room temperature, cells were washed once with 2 ml of phosphate-buffered saline (PBS), and 2 ml MEM with 10% FBS (for the Vero cell line) or RPMI 1640 with 10% FBS (for the BEAS-2B cell line) was added. At

time points p.i., cells were scraped in medium and resuspended, and aliquots were frozen until use. Differentiated NHBE cells were infected at an MOI of 0.2 or 2. Virus inoculum (100 $\mu$l) was applied apically after PBS wash (100 $\mu$l) followed by a 2-h incubation at 37°C. Inoculum was removed by three apical PBS washes. To collect virus for time points, differentiated medium without inducer (150 $\mu$l) was added to the apical chamber and cells were incubated for 10 min at 37°C. This step was repeated twice for each well (300-$\mu$l total). This apical supernatant was snap-frozen in liquid nitrogen and stored until use.

**Viral load and protection and vaccine efficacy.** All animal studies were approved by the Emory University Institutional Animal Care and Use Committee (protocol number 2001533) and carried out in accordance with recommendations in the Guide for Care and Use of Laboratory Animals of the National Institutes of Health, as well as local, state, and federal laws. Six- to eight-week-old female BALB/c mice (The Jackson Laboratory, Bar Harbor, ME) maintained under specific-pathogen-free conditions were intranasally (i.n.) infected with $1.6 \times 10^5$ FFU of virus per mouse. The left lung from each mouse was harvested for viral titer by FFU assay (described above) at days 1, 2, 4, 6, and 8 postinfection. For vaccine protection and efficacy assays, mice were vaccinated with various doses of either kRSV-A2 or kSRV-dNSh i.n. and challenged with either $1.6 \times 10^6$ PFU of RSV 12-35 (35) at 100 days after vaccination or $2 \times 10^6$ PFU of A2-line19F at 28 days after vaccination. For mice infected with $1 \times 10^5$ FFU vaccine virus and challenged 100 days postinfection, serum samples were collected on days 28, 42, 56, and 100 by mandibular bleeding. Lung peak viral loads postchallenge were measured on day 4 after challenge by plaque assay as described in reference 35. For all mouse experiments, *n* was 5 per group. Titers below the limit of detection were assigned half the value of the limit of detection.

**Microneutralization assay.** HEp-2 cells were seeded in 96-well plates to attain 70% confluence in 24 h. Heat-inactivated (56°C, 30 min) serum samples were 2-fold serially diluted in MEM and added to 50 to 100 FFU kRSV-A2 in an equal volume. The virus and serum mixture was incubated at 37°C for 1 h. Then, half of the serum-virus mixture was transferred onto HEp-2 cell monolayers in 96-well plates in duplicate, and plates were spinoculated at $2{,}000 \times g$ for 30 min at 4°C. Fluorescent foci were counted 36 h p.i. The 50% effective concentration ($EC_{50}$) was calculated using a nonlinear regression analysis with four-parameter fitting in GraphPad Prism version 6.0.

**NF-κB activation assay.** NF-κB activity was assayed according to the manufacturer's protocol (InvivoGen, San Diego, CA). Briefly, HEK-Blue-Null 1 cells were seeded at $5 \times 10^4$/well in a 96-well plate and infected with either kRSV-A2 or kRSV-dNSh or mock infected for 72 h. Supernatants were incubated with Quanti-Blue (InvivoGen, San Diego, CA) substrate prepared according to instructions for 1 to 3 h before reading optical density at 630 nm on a microplate reader (Bio-Tek, Winooski, VT).

**Statistical analysis.** Statistical analysis was performed using GraphPad Prism software version 6.0 (San Diego, CA). Data are represented as means with standard deviation (SDs). One-way and two-way analyses of variance (ANOVA) with Tukey's *post hoc* test with a $P$ value of 0.05 were used, as indicated. Student's $t$ test (unpaired, two-tailed) was used for Fig. 6A.

## ACKNOWLEDGMENTS

This work was supported by NIH grants 1R01AI087798 and 1U19AI095227 and by Emory University and Children's Healthcare of Atlanta funds.

We thank Edward Walsh for monoclonal antibody to RSV N protein and Michael Teng for antisera to RSV NS1 and NS2 proteins. We thank Ursula Buchholz and Karl-Klaus Conzelmann for BSR-T7/5 cells.

M.L.M. and Emory University are entitled to licensing fees derived from various agreements Emory has entered into related to products used in the research described in this paper. This study could affect his personal financial status. The terms of this agreement have been reviewed and approved by Emory University in accordance with its conflict of interest policies.

## REFERENCES

1. **Stockman LJ, Curns AT, Anderson LJ, Fischer-Langley G.** 2012. Respiratory syncytial virus-associated hospitalizations among infants and young children in the United States, 1997-2006. Pediatr. Infect. Dis. J. **31:**5–9. http://dx.doi.org/10.1097/INF.0b013e31822e68e6.
2. **Nair H, Nokes DJ, Gessner BD, Dherani M, Madhi SA, Singleton RJ, O'Brien KL, Roca A, Wright PF, Bruce N, Chandran A, Theodoratou E, Sutanto A, Sedyaningsih ER, Ngama M, Munywoki PK, Kartasasmita C, Simões EA, Rudan I, Weber MW, Campbell H.** 2010. Global burden of acute lower respiratory infections due to respiratory syncytial virus in young children: a systematic review and meta-analysis. Lancet **375:** 1545–1555. http://dx.doi.org/10.1016/S0140-6736(10)60206-1.
3. **Hall CB, Weinberg GA, Blumkin AK, Edwards KM, Staat MA, Schultz AF, Poehling KA, Szilagyi PG, Griffin MR, Williams JV, Zhu Y, Grijalva CG, Prill MM, Iwane MK.** 2013. Respiratory syncytial virus-associated hospitalizations among children less than 24 months of age. Pediatrics **132:**e341–e348. http://dx.doi.org/10.1542/peds.2013-0303.
4. **Collins PL, Melero JA.** 2011. Progress in understanding and controlling respiratory syncytial virus: still crazy after all these years. Virus Res. **162:** 80–99. http://dx.doi.org/10.1016/j.virusres.2011.09.020.
5. **Graham BS.** 2011. Biological challenges and technological opportunities for respiratory syncytial virus vaccine development. Immunol. Rev. **239:** 149–166. http://dx.doi.org/10.1111/j.1600-065X.2010.00972.x.
6. **Elliott J, Lynch OT, Suessmuth Y, Qian P, Boyd CR, Burrows JF, Buick R, Stevenson NJ, Touzelet O, Gadina M, Power UF, Johnston JA.** 2007. Respiratory syncytial virus NS1 protein degrades STAT2 by using the elongin-cullin E3 ligase. J. Virol. **81:**3428–3436. http://dx.doi.org/10.1128/JVI.02303-06.
7. **Goswami R, Majumdar T, Dhar J, Chattopadhyay S, Bandyopadhyay SK, Verbovetskaya V, Sen GC, Barik S.** 2013. Viral degradasome hijacks mitochondria to suppress innate immunity. Cell Res. **23:**1025–1042. http://dx.doi.org/10.1038/cr.2013.98.
8. **Ling Z, Tran KC, Teng MN.** 2009. Human respiratory syncytial virus nonstructural protein NS2 antagonizes the activation of beta interferon transcription by interacting with RIG-I. J. Virol. **83:**3734–3742. http://dx.doi.org/10.1128/JVI.02434-08.
9. **Lo MS, Brazas RM, Holtzman MJ.** 2005. Respiratory syncytial virus nonstructural proteins NS1 and NS2 mediate inhibition of Stat2 expression and alpha/beta interferon responsiveness. J. Virol. **79:**9315–9319. http://dx.doi.org/10.1128/JVI.79.14.9315-9319.2005.
10. **Ramaswamy M, Shi L, Varga SM, Barik S, Behlke MA, Look DC.** 2006. Respiratory syncytial virus nonstructural protein 2 specifically inhibits type I interferon signal transduction. Virology **344:**328–339. http://dx.doi.org/10.1016/j.virol.2005.09.009.
11. **Spann KM, Tran KC, Chi B, Rabin RL, Collins PL.** 2004. Suppression of the induction of alpha, beta, and lambda interferons by the NS1 and NS2 proteins of human respiratory syncytial virus in human epithelial cells and macrophages. J. Virol. **78:**4363–4369. http://dx.doi.org/10.1128/JVI.78.8.4363-4369.2004.
12. **Spann KM, Tran KC, Collins PL.** 2005. Effects of nonstructural proteins NS1 and NS2 of human respiratory syncytial virus on interferon regulatory factor 3, NF-kappaB, and proinflammatory cytokines. J. Virol. **79:** 5353–5362. http://dx.doi.org/10.1128/JVI.79.9.5353-5362.2005.
13. **Swedan S, Musiyenko A, Barik S.** 2009. Respiratory syncytial virus nonstructural proteins decrease levels of multiple members of the cellular interferon pathways. J. Virol. **83:**9682–9693. http://dx.doi.org/10.1128/JVI.00715-09.
14. **Hastie ML, Headlam MJ, Patel NB, Bukreyev AA, Buchholz UJ, Dave KA, Norris EL, Wright CL, Spann KM, Collins PL, Gorman JJ.** 2012. The human respiratory syncytial virus nonstructural protein 1 regulates type I and type II interferon pathways. Mol. Cell. Proteomics **11:**108–127. http://dx.doi.org/10.1074/mcp.M111.015909.
15. **Kotelkin A, Belyakov IM, Yang L, Berzofsky JA, Collins PL, Bukreyev A.** 2006. The NS2 protein of human respiratory syncytial virus suppresses the cytotoxic T-cell response as a consequence of suppressing the type I interferon response. J. Virol. **80:**5958–5967. http://dx.doi.org/10.1128/JVI.00181-06.
16. **Munir S, Hillyer P, Le Nouen C, Buchholz UJ, Rabin RL, Collins PL, Bukreyev A.** 2011. Respiratory syncytial virus interferon antagonist NS1 protein suppresses and skews the human T lymphocyte response. PLoS Pathog. **7:**e1001336. http://dx.doi.org/10.1371/journal.ppat.1001336.
17. **Munir S, Le Nouen C, Luongo C, Buchholz UJ, Collins PL, Bukreyev A.**

2008. Nonstructural proteins 1 and 2 of respiratory syncytial virus suppress maturation of human dendritic cells. J. Virol. **82:**8780–8796. http://dx.doi.org/10.1128/JVI.00630-08.

18. **Bitko V, Shulyayeva O, Mazumder B, Musiyenko A, Ramaswamy M, Look DC, Barik S.** 2007. Nonstructural proteins of respiratory syncytial virus suppress premature apoptosis by an NF-kappaB-dependent, interferon-independent mechanism and facilitate virus growth. J. Virol. **81:**1786–1795. http://dx.doi.org/10.1128/JVI.01420-06.
19. **Jin H, Cheng X, Traina-Dorge VL, Park HJ, Zhou H, Soike K, Kemble G.** 2003. Evaluation of recombinant respiratory syncytial virus gene deletion mutants in African green monkeys for their potential as live attenuated vaccine candidates. Vaccine **21:**3647–3652. http://dx.doi.org/10.1016/S0264-410X(03)00426-2.
20. **Jin H, Zhou H, Cheng X, Tang R, Munoz M, Nguyen N.** 2000. Recombinant respiratory syncytial viruses with deletions in the NS1, NS2, SH, and M2-2 genes are attenuated in vitro and in vivo. Virology **273:**210–218. http://dx.doi.org/10.1006/viro.2000.0393.
21. **Teng MN, Whitehead SS, Bermingham A, St. Claire M, Elkins WR, Murphy BR, Collins PL.** 2000. Recombinant respiratory syncytial virus that does not express the NS1 or M2-2 protein is highly attenuated and immunogenic in chimpanzees. J. Virol. **74:**9317–9321. http://dx.doi.org/10.1128/JVI.74.19.9317-9321.2000.
22. **Whitehead SS, Bukreyev A, Teng MN, Firestone CY, St Claire M, Elkins WR, Collins PL, Murphy BR.** 1999. Recombinant respiratory syncytial virus bearing a deletion of either the NS2 or SH gene is attenuated in chimpanzees. J. Virol. **73:**3438–3442.
23. **Luongo C, Winter CC, Collins PL, Buchholz UJ.** 2013. Respiratory syncytial virus modified by deletions of the NS2 gene and amino acid S1313 of the L polymerase protein is a temperature-sensitive, live-attenuated vaccine candidate that is phenotypically stable at physiological temperature. J. Virol. **87:**1985–1996. http://dx.doi.org/10.1128/JVI.02769-12.
24. **Teng MN.** 2012. The non-structural proteins of RSV: targeting interferon antagonists for vaccine development. Infect. Disord. Drug Targets **12:**129–137. http://dx.doi.org/10.2174/187152612800100170.
25. **Lin YH, Deatly AM, Chen W, Miller LZ, Lerch R, Sidhu MS, Udem SA, Randolph VB.** 2006. Genetic stability determinants of temperature sensitive, live attenuated respiratory syncytial virus vaccine candidates. Virus Res. **115:**9–15. http://dx.doi.org/10.1016/j.virusres.2005.06.013.
26. **Malkin E, Yogev R, Abughali N, Sliman J, Wang CK, Zuo F, Yang CF, Eickhoff M, Esser MT, Tang RS, Dubovsky F.** 2013. Safety and immunogenicity of a live attenuated RSV vaccine in healthy RSV-seronegative children 5–24 months of age. PLoS One **8:**e77104. http://dx.doi.org/10.1371/journal.pone.0077104.
27. **Crowe JE, Jr, Bui PT, Siber GR, Elkins WR, Chanock RM, Murphy BR.** 1995. Cold-passaged, temperature-sensitive mutants of human respiratory syncytial virus (RSV) are highly attenuated, immunogenic, and protective in seronegative chimpanzees, even when RSV antibodies are infused shortly before immunization. Vaccine **13:**847–855. http://dx.doi.org/10.1016/0264-410X(94)00074-W.
28. **Mueller S, Papamichail D, Coleman JR, Skiena S, Wimmer E.** 2006. Reduction of the rate of poliovirus protein synthesis through large-scale codon deoptimization causes attenuation of viral virulence by lowering specific infectivity. J. Virol. **80:**9687–9696. http://dx.doi.org/10.1128/JVI.00738-06.
29. **Burns CC, Shaw J, Campagnoli R, Jorba J, Vincent A, Quay J, Kew O.** 2006. Modulation of poliovirus replicative fitness in HeLa cells by deoptimization of synonymous codon usage in the capsid region. J. Virol. **80:**3259–3272. http://dx.doi.org/10.1128/JVI.80.7.3259-3272.2006.
30. **Coleman JR, Papamichail D, Skiena S, Futcher B, Wimmer E, Mueller S.** 2008. Virus attenuation by genome-scale changes in codon pair bias. Science **320:**1784–1787. http://dx.doi.org/10.1126/science.1155761.
31. **Nakamura Y, Gojobori T, Ikemura T.** 2000. Codon usage tabulated from international DNA sequence databases: status for the year 2000. Nucleic Acids Res. **28:**292. http://dx.doi.org/10.1093/nar/28.1.292.
32. **Hotard AL, Shaikh FY, Lee S, Yan D, Teng MN, Plemper RK, Crowe JE, Jr, Moore ML.** 2012. A stabilized respiratory syncytial virus reverse genetics system amenable to recombination-mediated mutagenesis. Virology **434:**129–136. http://dx.doi.org/10.1016/j.virol.2012.09.022.
33. **Wright PF, Ikizler MR, Gonzales RA, Carroll KN, Johnson JE, Werkhaven JA.** 2005. Growth of respiratory syncytial virus in primary epithelial cells from the human respiratory tract. J. Virol. **79:**8651–8654. http://dx.doi.org/10.1128/JVI.79.13.8651-8654.2005.
34. **Zhang L, Peeples ME, Boucher RC, Collins PL, Pickles RJ.** 2002. Respiratory syncytial virus infection of human airway epithelial cells is polarized, specific to ciliated cells, and without obvious cytopathology. J. Virol. **76:**5654–5666. http://dx.doi.org/10.1128/JVI.76.11.5654-5666.2002.
35. **Stokes KL, Chi MH, Sakamoto K, Newcomb DC, Currier MG, Huckabee MM, Lee S, Goleniewska K, Pretto C, Williams JV, Hotard A, Sherrill TP, Peebles RS, Jr, Moore ML.** 2011. Differential pathogenesis of respiratory syncytial virus clinical isolates in BALB/c mice. J. Virol. **85:**5782–5793. http://dx.doi.org/10.1128/JVI.01693-10.
36. **Heinze B, Frey S, Mordstein M, Schmitt-Gräff A, Ehl S, Buchholz UJ, Collins PL, Staeheli P, Krempl CD.** 2011. Both nonstructural proteins NS1 and NS2 of pneumonia virus of mice are inhibitors of the interferon type I and type III responses in vivo. J. Virol. **85:**4071–4084. http://dx.doi.org/10.1128/JVI.01365-10.
37. **Bossert B, Marozin S, Conzelmann KK.** 2003. Nonstructural proteins NS1 and NS2 of bovine respiratory syncytial virus block activation of interferon regulatory factor 3. J. Virol. **77:**8661–8668. http://dx.doi.org/10.1128/JVI.77.16.8661-8668.2003.
38. **Valarcher JF, Furze J, Wyld S, Cook R, Conzelmann KK, Taylor G.** 2003. Role of alpha/beta interferons in the attenuation and immunogenicity of recombinant bovine respiratory syncytial viruses lacking NS proteins. J. Virol. **77:**8426–8439. http://dx.doi.org/10.1128/JVI.77.15.8426-8439.2003.
39. **Schlender J, Bossert B, Buchholz U, Conzelmann KK.** 2000. Bovine respiratory syncytial virus nonstructural proteins NS1 and NS2 cooperatively antagonize alpha/beta interferon-induced antiviral response. J. Virol. **74:**8234–8242. http://dx.doi.org/10.1128/JVI.74.18.8234-8242.2000.
40. **Swedan S, Andrews J, Majumdar T, Musiyenko A, Barik S.** 2011. Multiple functional domains and complexes of the two nonstructural proteins of human respiratory syncytial virus contribute to interferon suppression and cellular location. J. Virol. **85:**10090–10100. http://dx.doi.org/10.1128/JVI.00413-11.
41. **Teng MN, Collins PL.** 1999. Altered growth characteristics of recombinant respiratory syncytial viruses which do not produce NS2 protein. J. Virol. **73:**466–473.
42. **Vitiello M, Galdiero M, Finamore E, Galdiero S, Galdiero M.** 2012. NF-kappaB as a potential therapeutic target in microbial diseases. Mol. Biosyst. **8:**1108–1120. http://dx.doi.org/10.1039/c2mb05335g.
43. **Mueller S, Coleman JR, Papamichail D, Ward CB, Nimnual A, Futcher B, Skiena S, Wimmer E.** 2010. Live attenuated influenza virus vaccines by computer-aided rational design. Nat. Biotechnol. **28:**723–726. http://dx.doi.org/10.1038/nbt.1636.
44. **Yang C, Skiena S, Futcher B, Mueller S, Wimmer E.** 2013. Deliberate reduction of hemagglutinin and neuraminidase expression of influenza virus leads to an ultraprotective live vaccine in mice. Proc. Natl. Acad. Sci. U. S. A. **110:**9481–9486. http://dx.doi.org/10.1073/pnas.1307473110.
45. **Hershberg R, Petrov DA.** 2008. Selection on codon bias. Annu. Rev. Genet. **42:**287–299. http://dx.doi.org/10.1146/annurev.genet.42.110807.091442.
46. **Ikemura T.** 1985. Codon usage and tRNA content in unicellular and multicellular organisms. Mol. Biol. Evol. **2:**13–34.
47. **Najafabadi HS, Goodarzi H, Salavati R.** 2009. Universal function-specificity of codon usage. Nucleic Acids Res. **37:**7014–7023. http://dx.doi.org/10.1093/nar/gkp792.
48. **Tuller T, Carmi A, Vestsigian K, Navon S, Dorfan Y, Zaborske J, Pan T, Dahan O, Furman I, Pilpel Y.** 2010. An evolutionarily conserved mechanism for controlling the efficiency of protein translation. Cell **141:**344–354. http://dx.doi.org/10.1016/j.cell.2010.03.031.
49. **Qian W, Yang JR, Pearson NM, Maclean C, Zhang J.** 2012. Balanced codon usage optimizes eukaryotic translational efficiency. PLoS Genet. **8:**e1002603. http://dx.doi.org/10.1371/journal.pgen.1002603.
50. **Zhou M, Guo J, Cha J, Chae M, Chen S, Barral JM, Sachs MS, Liu Y.** 2013. Non-optimal codon usage affects expression, structure and function of clock protein FRQ. Nature **495:**111–115. http://dx.doi.org/10.1038/nature11833.
51. **Pechmann S, Frydman J.** 2013. Evolutionary conservation of codon optimality reveals hidden signatures of cotranslational folding. Nat. Struct. Mol. Biol. **20:**237–243. http://dx.doi.org/10.1038/nsmb.2466.